



TURBULENT FLOW ANALYSIS IN AUXILIARY CROSS-FLOW RUNNER OF A PROTO X-3 BIOENERGY MICRO GAS TURBINE USING RNG k - ϵ TURBULENCE MODEL

Steven Darmawan^{1,2}, Ahmad Indra Siswantara¹, Budiarmo¹, Asyari Daryus^{1,3}, Agus Tri Gunawan¹, Achmad Bayu Wijayanto¹ and Harto Tanujaya²

¹Department of Mechanical Engineering, Universitas Indonesia, Depok, Jawa Barat, Indonesia

²Department of Mechanical Engineering, Universitas Tarumanagara. Jl. Let.Jen S. Parman No.1 Jakarta. Indonesia

³Department of Mechanical Engineering. Universitas Darma Persada. Jl. Radin Inten II, Pondok Kelapa. Jakarta Indonesia

E-Mail: stevend@ft.untar.ac.id

ABSTRACT

Simple and wide range application of cross-flow runner has lead its application to a Proto X-3 Bioenergy Micro Gas Turbine (MGT) that has been developed. The MGT is a dual-stage radial compressor-turbine type. Furthermore, highly turbulent flow inside the cross-flow fan need accurate analysis. CFD method with RNG k - ϵ choosen based on models characteristics. This paper analyzed the flow inside the fan based on the experimental data of the MGT and the result represented by several parameters of turbulent flow. The simulation condition were assumed to be isothermal due to the small temperature difference with the tubulent Prandtl number $Pr_t = 1$. The result shows several specific vortex inside the runner. Recirculation flow cthat caused the eccentric vortex occurs at the inner side while the throughflow occurs at the outside of the fan. The mass flow rate conducted by CFD simulation shows a good agreement with the actual mass flow rate of the cross-flow runner. The results that presented by velocity magnitude, absolute pressure, eddy dissipation, and turbulence kinetic energy shows a realistic on each turbulent parameter based on they trends. This results shows that the method used is prospective to be applied both on analysis or design of the cross-flow runner.

Keywords: cross-flow runner, MGT, turbulent flow, RNG k - ϵ turbulence model, recirculation vortex.

INTRODUCTION

Cross-flow runner (CFR, hereafter) is a atmospheric radial turbine that generates power by converting kinetic energy to mechanical energy which based on Banki turbine (cross-flow turbine) [1]. CFR system consist of two main components; the runner itself and the nozzle with square cross-section. CFR design based on three main characteristics; simple construction, low-cost, and maximum efficiency and has been prospected as Renewable Energy Resources (RES) for under 3MW hydroelectric generator system [2], [3]. This characteristics has lead the applications of CFR as power extractor of a Proto X-3 Bioenergy Micro Gas Turbine (MGT) prototype that has been developed which is a dual-stage compressor-turbine [4]. The CFR was driven by the inlet air of the first stage compressor. The high flow air to first stage made it possible to drive the cross-flow fan. Basically, MGT is developed for small power generation upto 200 kW [5], [6]. Some of the advantages of this MGT are high power to weight ratio, high tolerance to many kind of liquid and gaseous fuels and biofuels has made this prime mover suitable to be used in Zero-Energy-Building-based [7-10].

During the operation, as a turbomachine, the suction and discharge of CFR occurs radially, generated highly turbulent flow for recirculating and reserve flow [11]. Many experimental and numerical analysis shows the flow complexity of CFR. Experimental study by numbers of researcher has lead to description of two main vortex inside the CFR; throughflow at the outside region and recirculation flow at the inside region [12-17].

Handling and costly experiment as well as the accuration has made numerical method also conducted on last decade with many turbulence model. Kaniecki use RNG k - ϵ found the throughflow as well as the recirculation flow [18]. Cheng use STD k - ϵ in numerical analysis the flow of CFR [19]. RNG k - ϵ also uses by Toffolo (2005) [16]. Hirata et.al in 2008 use STD k - ϵ [20]. The current numerical analysis by Sun et.al also RNG k - ϵ turbulence model for more detailed flow [17]. These numerical results show there are two main vortexes occur in CFR; the eccentric vortex at recirculation region and vortex in the throughflow region. Since the flow inside the CFR is undoubtly turbulent, flow analysis of turbulent flow with suitable turbulence model is needed to analysis and can be used for future development of the CFR system. Despite the STD k - ϵ as the most widely used turbulence model, this model also reported since that model is overpredicts the dissipation rate [21-24]. RNG k - ϵ turbulence model developed by Yakhot & Orszag [25] for recirculating flow has became alternatives to predict such flows [26], [27].

The aim of this paper is to analyze numerically the flow inside the cross-flow runner with RNG k - ϵ turbulence model since this model is developed to such flow. The turbulent momentum diffusivity and turbulent thermal diffusivity is also assumed to be equal ($Pr_t = 1$) and the deafult constant to the Yakhot & Orszag model was used. Optimal flow characteristics of cross-flow runner on Proto X-3 can be used to optimized the system to be a compact prime mover system.



RESEARCH METHODOLOGY

Experimental Set-up

Experiment on Proto X-3 Bioenergy MGT was done according to experiment schematic on Figure-1. According Figure-1, the CFR in which represented by component No.6, installed inside an acrylic casing. The rest of the components on Figure-1 is not discussed in this paper. The CFR is driven by the inlet pre-compressed air of 1st stage compressor. This mechanism clarifies the definition of the CFR. Measurement and acquisition data have been done to several characteristics parameters of MGT.

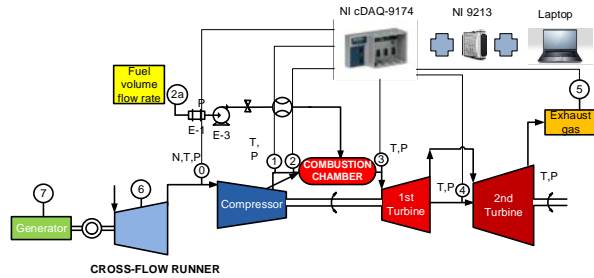


Figure-1. Experimental schematic of prototype.

Numerical Analysis Set-up

Numerical analysis only done on the CFR since the component is now become our research interest. Cross-flow runner was operated by air at first stage compressor inlet as can be seen on Figure-1. Due to the small temperature difference between inlet and outlet of the CFR, the simulation condition is assumed isothermal. The wall is assumed zero-roughness. Computational grid shown on Figure-2, is a quasi three-dimensional grid, consists of 299 x 130 x 3 cells. Grid dependency was conducted to several grid numbers, from coarse to finer which was resulting consistent result. The sliding mesh is used for the rotational move of the runner. Figure-2 also shows the two stage of runner operation.

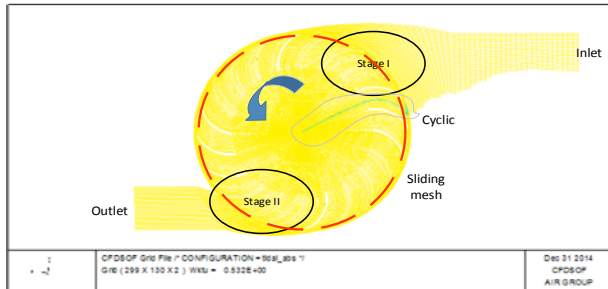


Figure-2. Computational grid of cross-flow fan.

In order to represent the flow phenomena inside the runner, the runner's cross-section is configured to be 8 zones, from 0° to 360° as shown on Figure-3. With this configuration, it is able to describe the special flow phenomena or special vortex that occurs during the

simulation. Zone I and II represent the inlet section and zone V and VI represent the outlet section.

The results of CFD simulation are described into several turbulent flow quantities; velocity magnitude and total pressure. Since the flow inside the runner undoubtedly turbulent, turbulence quantities are described as well; eddy dissipation, effective viscosity, and turbulent kinetic energy.

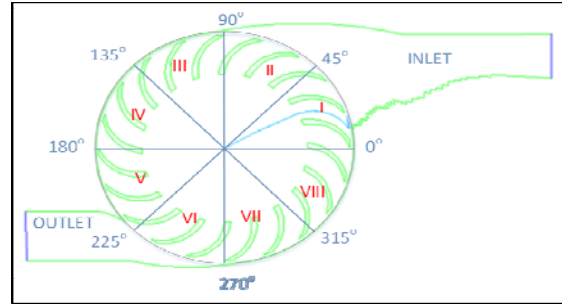


Figure-3. Flow zone configuration.

Governing Equations

Averaging on Navier-Stokes equations – like on the other RANS-based turbulence model, has caused the Reynolds stress term. The Reynolds stress $\rho \overline{u_i u_j}$ (kg.m/s²) also correlates the turbulent viscosity. Momentum transfer caused by turbulent flow modeled by the use of eddy viscosity concept. In turbulent flow, turbulent viscosity ν_T (m²/s) occur as additional viscosity term and has caused the increasing of total viscosity ν_{eff} (m²/s). The Reynolds stress can be defined as velocity gradient [28], [29]. Total viscosity of the flow described by [24].

$$\rho \overline{u_i u_j} = \frac{\rho}{Pr} \overline{u_i u_j} + (\nu_T \left[\frac{\partial u_i}{\partial x_j} + \frac{\partial u_j}{\partial x_i} \right]) \tag{1}$$

$$\nu_{eff} = \nu_T + \nu \tag{2}$$

$$\nu_T = C_\mu \frac{k^2}{\epsilon} \tag{3}$$

Transferred energy from large scale eddies to small scale eddies, and how the energy is dissipated in RNG $k-\epsilon$ governed by Kolmogorov theorem [25], [30], [31]. In turbulent flow, amount of energy supplied can be assumed equal to be dissipated on certain rate. Therefore, this energy rate is small compared to energy dissipated [32]. In Kolmogorov theorem, where velocity fluctuations tends to be universal, the amount of energy assumed only depends on turbulent dissipation rate (ϵ) and length scale (l) [25], [33].

$$E(k) = C_k \epsilon^{-2/3} k^{-5/3} \tag{4}$$

The RNG $k-\epsilon$ turbulence model uses the normalized Navier-Stokes equation where acceleration and force governed according to [25], [34]:

$$\frac{\partial \mathbf{u}}{\partial t} = (\mathbf{u} \cdot \nabla) \mathbf{u} = \mathbf{f} - \frac{1}{\rho} \nabla p + \nu_T \nabla^2 \mathbf{u} \tag{5}$$



Inverse-Turbulent Prandtl number, α described the ratio between thermal diffusivity and turbulent viscosity according to: [25] [35] [36]

$$\alpha = \frac{\nu_t}{\nu} \quad (6)$$

In general fluids, the heat transfer is dominated by molecular diffusion, the thermal resistance is distributed over the entire cross-section, and the turbulent Prandtl number, α , assume equal to one [37]. RNG $k-\epsilon$ turbulence models is a RANS-based turbulence model with two transport equation; k (turbulence kinetic energy) and ϵ (turbulent dissipation). RNG $k-\epsilon$ turbulence model applied since this model is suitable to predict the recirculating flows that dominantly occur in crossflow runner [24-27]. RNG $k-\epsilon$ use here is an in-house codes from the CFDSOFT CFD-software.

Transport equation of k [25]

$$\frac{\partial k}{\partial t} + (U_j \nabla_j)k = 0.8(235)^{1/2} \nu \nabla^2 k - \epsilon + \frac{\partial}{\partial x_i} \left(\alpha \nu_t \nabla_i k \right) \quad (7)$$

Transport equation of ϵ [25]

$$\frac{\partial \epsilon}{\partial t} = -1.069 \frac{\epsilon}{k} U_j \nabla_j k - 1.7215 \frac{\epsilon^2}{k} + \frac{\partial}{\partial x_i} \left(\alpha \nu_t \nabla_i \epsilon \right) \quad (8)$$

RESULTS

Experiment Result

The results shows below obtained from the experimental data of the Proto X-3 Bioenergy MGT that has been designed and developed. The idea to shows almost the whole parameters of the Prototype is to state that the parameters that is used for the CFD simulation of the cross-flow fan is obtained at the stable condition of the MGT. The 1st stage of compressor and turbine is a radial turbocharger. Such condition is represented by turbine inlet temperature to the running time as shown on Figure-4.

- Ambient temperature : 33°C
- Shaft speed (1st stage) : 69477 RPM
- Air flow rate (1st stage) : 0,1663 kg/s
- T1 (1stage compressor inlet) : 83,78°C
- Pressure ratio (1st stage comp.) : 1,45
- T3 (Turbine Inlet Temperature - TIT) : 707,8°C
- Cross-flow runner speed : 1500 RPM

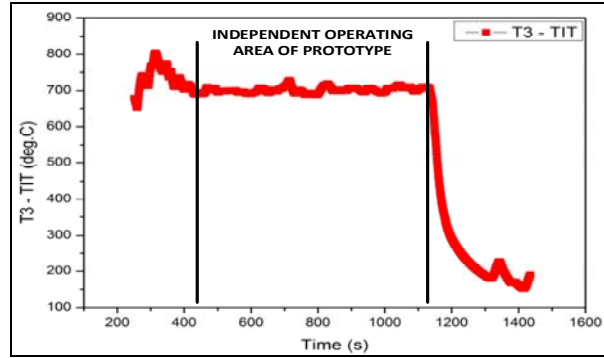


Figure-4. Representation of prototype running data.

First stage inlet velocity from the inlet air flow rate:

$$V_1 = 46,667 \text{ m/s}$$

Cross-section area of the inlet cross-flow runner:

$$A = 0,003364 \text{ m}^2$$

Reynolds number Re at cross-flow inlet; ρ = density of air, μ = dynamic viscosity

$$Re = \frac{\rho V D_H}{\mu}$$

With hydraulic diameter D_H ;

$$D_H = \frac{4A}{P}, \text{ With } A = \text{cross-sectional area} = 0,003364 \text{ m}^2$$

$$P = \text{wetted perimeter} = 2(0,099 \text{ m} + 0,083 \text{ m}) = 0,27 \text{ m}$$

$$D_H = 0,0828 \text{ m}$$

Then

$$Re = \frac{0,4363 \text{ kg/m}^3 \times 46,667 \text{ m/s} \times 0,0828 \text{ m}}{3,64 \times 10^{-4} \text{ N.s/m}^2} = 80,900$$

From the numerical procedure, the flow rate of runner at inlet and outlet is 0,1536 m³/s, the torque at the sliding mesh wall is 18,55 Nm resulting 2,91 kW. Validation of the mass flow rate to the 1st stage compressor inlet underpredict 5,7% from the 1st stage compressor map (this compressor map got by request from turbocharger manufacturer).

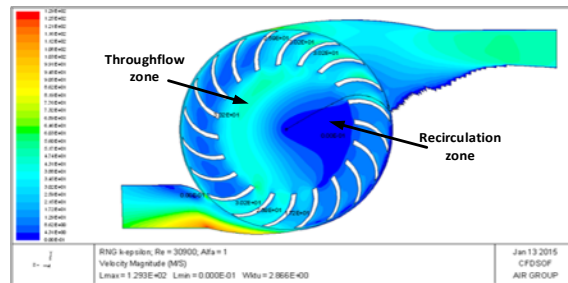


Figure-5. Velocity magnitude.



www.arpnjournals.com

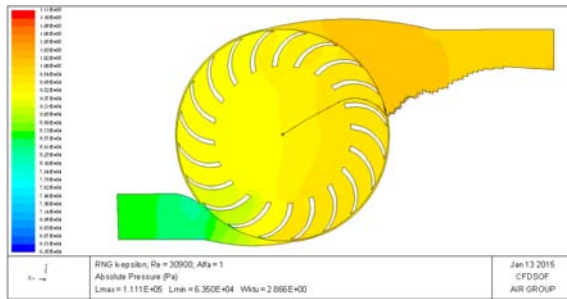


Figure-6. Absolute static pressure.

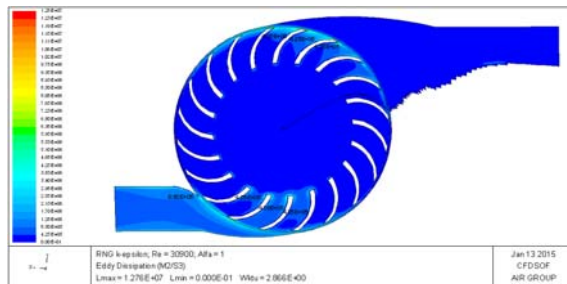


Figure-7. Eddy dissipation.

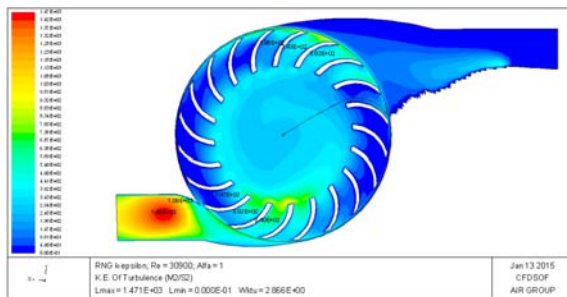


Figure-8. Turbulence kinetic energy.

Velocity magnitude of cross-flow runner shows that two dominant vortices occur inside the runner. The forced vortex, occurs in throughflow where the fluid passed the 1st inlet to the 2nd inlet. At the other side of the throughflow zone, the area with less-fluid concentration forms the eccentric vortex in recirculated flow. This eccentric vortex occurs at zone I and VIII or at $315^\circ - 45^\circ$ according to Figure-2, and Figure-3. This result also confirms that eccentric vortex is caused by recirculation flow.

Many previous papers show that this eccentric vortex is dominant flow at runner and decreasing the runner performance, as concluded by Sun et.al (2015) and Choi et.al (2007) [17], [38]. The *RNG k- ϵ* turbulence model shows this vortex fairly in figures above. Recirculation vortex occurs at the inner side at zone VII and VIII while the throughflow vortex at the outer side of the runner at zone III and IV. This zone range also gained by Hirata et.al where that the recirculation flow that caused eccentric vortex occurs at $330^\circ - 360^\circ$ region [20]. In line with the velocity prediction, the result of predicted

absolute static pressure is shown on Figure 6. The figure describes that pressure drop occurs in operated condition of the runner about 14300 Pa (0,143 bar). This drop is suspected to the occurrence of the eccentric vortex as shown on velocity magnitude contour, as well as the Boussinesq hypothesis about the additional turbulent viscosity in eq. (3). As the lower velocity due to eccentric vortex in figure 5, the pressure in recirculation zone (zone VII and VIII) higher than at zone III and IV as shown on Figure-6.

Figure-7 shows the eddy dissipation on cross-flow runner. The turbulence dissipate dominantly at the area around the blade at inlet zone and at outlet zone and nearly zero at circulation area at zone VII and VIII; throughflow zone and the recirculation zone of the runner. Since dissipation is a turbulence characteristic that represent turbulent decaying in lower velocity, the numerical result shows fairly. This is according to the velocity magnitude contour which shows that the high velocity inside the runner while lower velocity occur at area around the blades, and cause the flow dissipates.

Turbulence kinetic energy contour is shown on Figure-8. Contour of turbulence kinetic energy shows maximum at the outlet side of the system where recirculation flow occurred caused by cross-sectional change. Special phenomena occurs at the center of the runner, area of the throughflow and the recirculation flow. Leaving the 1st inlet stage with lower viscosity, the turbulent kinetic energy increased gradually. Another phenomena occur at recirculation zone, where the turbulence kinetic energy much higher than at the throughflow zone. This suspected due to velocity fluctuation of the recirculation flow since turbulence kinetic energy represents the velocity fluctuation on all direction; u , v , and w respectively.

CONCLUSIONS

CFD simulation is deduced with *RNG k- ϵ* turbulence model with 5,7% flow rate underprediction to the actual flow rate. Velocity magnitude of cross-flow runner shows that two dominant vortices occur inside the runner, the forced vortex and eccentric vortex. The forced vortex zone occurs in throughflow (zone III and IV) and the eccentric vortices occur at the other sides (Zone VII and VIII). Pressure drop occurs in operated condition of the runner about 14300 Pa which suspected by the occurrence of the eccentric vortex.

The turbulence dissipate dominantly at the area around the blade at inlet zone and at outlet zone and nearly zero at circulation area; throughflow zone and the recirculation zone of the runner. Contour of turbulence kinetic energy shows maximum at the outlet side of the system where recirculation flow occurs caused by cross-sectional change.

It can be concluded that The *RNG k- ϵ* turbulence model is adequate to describe vortices, especially for cross-flow runner; ie. throughflow and recirculating vortex and for further development of the CFR design.



ACKNOWLEDGEMENT

The authors would like to thanks DRPM Universitas Indonesia for funding this research through "Hibah Unggulan Perguruan Tinggi 2015".

REFERENCES

- [1] C. Mockmore and F. Merryfield, "The Banki Water Turbine," Bulletin Series, no. 25, February 1949.
- [2] S. Khosrowpanah and A. Fiuzat, "Experimental Study of Cross-Flow Turbine," J. Hydraulic Eng., vol. 114, pp. 299-314, 1988.
- [3] V. Sammartano, C. Arico, A. Carravetta and O. Fecarotta, "Banki-Michell Optimal Design by Computational Fluid Dynamics Testing and Hydrodynamic Analysis," Energies, vol. 6, pp. 2362-2385, 2013.
- [4] A. I. Siswantara, Budiarto and S. Darmawan, "Investigation of Inverse-Turbulent-Prandtl number with Four RNG k- ϵ Turbulence Models on Compressor Discharge Pipe of Bioenergy Micro Gas Turbine," in International Meeting in Advance Thermofluids (IMAT) 7 2014, Kuala Lumpur, 2014.
- [5] A. I. Siswantara, S. Darmawan and O. Purba, "Combustion Analysis of Proto X-2 Bioenergy Micro Gas Turbine with Diesel-Bioethanol blends," in Quality in Research (QiR) 2013, Yogyakarta.
- [6] A. Huicochea, W. Rivera, G. Guitierrez-Urueta and J. C. Bruno, "Thermodynamics analysis of a trigeneration system consisting of a micro gas turbine and a double effect absorption chiller," Applied Thermal Engineering, vol. 31, pp. 3347-3353, 2011.
- [7] F. Basrawi, T. Yamada and S. Obara, "Theoretical analysis of performance of a micro gas turbine co/trigeneration system for residential buildings in a tropical region," Energy and Buildings, vol. 67, pp. 108-117, 2013.
- [8] K. Sim, B. Koo, C. H. Kim and T. H. Kim, "Development and performance measurement of micro-power pack using micro-gas turbine driven automotive alternators," Applied Energy, vol. 102, pp. 309-319, 2013.
- [9] I. Gokalp and E. Lebas, "Alternative fuels for industrial gas turbines (AFTUR)," Applied Thermal Engineering, vol. 24, pp. 1655-1663, 2004.
- [10] M. Prussi, D. Chiaramonti, G. Riccio, F. Martelli and L. Pari, "Straight vegetable oil use in Micro-Gas Turbines: System adaptation and testing," Applied Energy, vol. 89, pp. 287-295, 2012.
- [11] P. R. Tuckey, "The aerodynamics and performance of a cross flow fan," Durham University, Durham, 1983.
- [12] S. Murata and K. Nisihara, "An experimental study of cross flow fan," Bulletin of JSME, vol. 19, no. 129, 1976.
- [13] S. Murata, T. Ogawa, I. Shimizu, K. Nisihara and K. Kinoshita, "A study of cross flow fan with inner guide apparatus," JSME, vol. 21, no. 154, 1978.
- [14] T.-A. Kim, D.-W. Kim, S.-K. Park and Y. J.-Kim, "Performance of a cross-flow fan with various shapes of a rearguider and exit duct," Journal of Mechanical Science and Technology, vol. 22, pp. 1876-1882, 2008.
- [15] Y. J. Kim, "Flow Characteristics in a Cross-Flow Fan with Various Design Parameters," in The 4th International Symposium on Fluid Machinery and Fluid Engineering, Beijing, China, 2008.
- [16] A. Toffolo, "On the theoretical link between design parameters and performance in cross-flow fans: a numerical and experimental study," Computers & Fluids, vol. 34, pp. 49-66, 2005.
- [17] K. Sun, H. Ouyang, J. Tian, Y. Wu and Z. Du, "Experimental and numerical investigations on the eccentric vortex of the cross flow fans," International Journal of Refrigeration, vol. 50, pp. 146-155, 2015.
- [18] M. Kaniecki, "Modernization of the outflow system of cross-flow turbines," Task Quarterly, vol. 6, no. 4, pp. 601-608, 2002.
- [19] W. T. Cheng, "Experimental and numerical analysis of a crossflow fan," Master Thesis - Naval Postgraduate School, California, 2003.
- [20] K. Hirata, Y. Iida, A. Takushima and J. Funaki, "Instantaneous pressure measurement on a rotating blade of a cross-flow impeller," Journal of Environment and Engineering, vol. 3, no. 2, 2008.
- [21] B. Launder and D. Spalding, "The Numerical Computation of Turbulent Flows," Computer Methods in Applied Mechanics and Engineering, vol. 3, pp. 269-289, 1974.
- [22] B. Lakshminarayana, Fluid Dynamics and Heat Transfer of Turbomachinery, John Wiley & Sons, Inc., 1996.
- [23] E. M. Marshall and A. Bakker, "Computational Fluid Mixing - Technical Notes," Fluent Inc., Lebanon, NH, 2001.



www.arpnjournals.com

- [24] TM-107, "Introduction to the Renormalization Group Method and Turbulence Modeling," Fluent Inc., Lebanon, 1993.
- [25] V. Yakhot and S. A. Orszag, "Renormalization Group Analysis of Turbulence. I. Basic Theory," *Journal of Scientific Computing*, vol. 1, no. 1, pp. 3-51, 1986.
- [26] H. Versteeg and W. Malalasekara, *An Introduction to Computational Fluid Dynamics, The Finite Volume Method*, 2 ed., Essex: Pearson Educational Limited, 2007.
- [27] S. Thangam and C. Speziale, "Turbulent Flow Past a Backward-Facing Step: A Critical Evaluation of Two-Equation Models," *AIAA Journal*, vol. 30, no. 5, 1992.
- [28] S. Lam, "On The RNG Theory of Turbulence," *Physics of Fluids A*, vol. 4, pp. 1007-1017, 1992.
- [29] E. M. Marshall and A. Bakker, *Computational Fluid Mixing*, Lebanon, New Hampshire: John Wiley & Sons, Inc., 2003.
- [30] C. Speziale, R. So and B. Younis, "On the prediction of turbulent secondary flows," Hampton, Virginia, 1992.
- [31] A. Escue and J. Cui, "Comparison of Turbulence Models in Simulating Swirling Pipe Flows," *Applied Mathematic Modelling*, vol. 34, pp. 2840-2849, 2010.
- [32] H. Tennekes and J. Lumley, *A First Course In Turbulence*, 3 rd ed., MIT Press, 1974.
- [33] V. Yakhot, S. Orszag, S. Thangam, T. Gatski and C. Speziale, "Development of turbulence model for shear flows by a double expansion technique," *Phys. Fluid A*, vol. 4, no. 7, pp. 1510-1520, 1992.
- [34] B. R. Munson, D. F. Young, T. H. Okiishi and W. W. Huebsch, *Fundamentals of fluid mechanics*, 6th ed., John Wiley & Sons, Inc., 2009.
- [35] Budiarso, A. I. Siswantara, S. Darmawan and H. Tanujaya, "Inverse-turbulent Prandtl number effects on Reynolds number of RNG k- ϵ turbulence model on cylindrical curved-pipe," *Applied Mechanics and Materials*, vol. 758, pp. 35-44, 2015.
- [36] S. Darmawan, Budiarso and A. I. Siswantara, "CFD Investigation Of Standard k- ϵ and RNG k- ϵ Turbulence Model In Compressor Discharge Of Proto X-2 Bioenergy Micro Gas Turbine," in *The 8th Fluid and Thermal Energy Conversion (FTEC) 2013*, Semarang, 2013.
- [37] F. Chen, X. Huai, J. Cai, X. Li and R. Meng, "Investigation on the applicability of turbulent-Prandtl-number models for the liquid lead-bismuth eutectic," *Nuclear Engineering and Design*, vol. 257, pp. 128-133, 2013.
- [38] Y. Choi, J. Lim, Y. Kim and Y. Lee, "CFD analysis for the performance of cross-flow hydraulic turbine with the variation of blade angle," in *New Trends in Fluid Mechanics Research - The 5th International Conference on Fluid Mechanics*, Shanghai, China, 2007.
- [39] W. Meier, X. Duan and P. Weigand, "Reaction zone structures and mixing characteristics of partially premixed swirling CH₄/air flames in a gas turbine model combustor," *Proceedings of the Combustion Institute*, vol. 30, pp. 835-842, 2005.